

# Al(NO<sub>3</sub>)<sub>3</sub>/SiO<sub>2</sub> Synthesized from Rice Husk Ash Increases Isomer Separation Efficiency of Natural Beta-Caryophyllene

Arif Setiawansyah<sup>1,\*</sup> , Sella Permata<sup>2</sup>, Jeni Erliyana<sup>2</sup>, Yully Septiana<sup>2</sup>, Wahyu Kurniawan<sup>2</sup>, Yulius Evan Christian<sup>3</sup>, Anggi Utama Putri<sup>2</sup>, Yovi Pranata<sup>2</sup>, Khairunnisa Khairunnisa<sup>4</sup>, Muhammad Al Muttaqii<sup>5</sup> , Reva Edra Nugraha<sup>6,7</sup> , Abdul Aziz<sup>8,\*</sup> 

<sup>1</sup> Center of Natural Product Extract Laboratory, Akademi Farmasi Cendikia Farma Husada, Bandar Lampung, Indonesia; setiawansyah@akfarcefada.ac.id (A.S.);

<sup>2</sup> Faculty of Pharmacy, Kader Bangsa University, Palembang, Indonesia; sellapermata500@gmail.com (SP), jenierliyana@gmail.com (J.E.); yullyseptiani123@gmail.com (Y.S.); wahyukurniawan12032002@gmail.com (W.K.); anggyutama@gmail.com (A.U.P.); yovipranata72@gmail.com (Y.P.);

<sup>3</sup> Universitas Katolik Atma Jaya, Jakarta, Indonesia; yulius.christian@atmajaya.ac.id;

<sup>4</sup> Department of Pharmacy, STIK Siti Khadijah, Palembang, Indonesia; akhoirunnisa976@gmail.com;

<sup>5</sup> Research Center for Chemistry, National Research and Innovation Agency (BRIN-Indonesia), South Tangerang, Indonesia; almuttaqiimhammad@gmail.com;

<sup>6</sup> Department of Chemical Engineering, Faculty of Engineering, Universitas Pembangunan Nasional "Veteran" Jawa Timur, Surabaya, East Java, Indonesia; reva.edra.tk@upnjatim.ac.id;

<sup>7</sup> Low Carbon Technologies Research Center, Universitas Pembangunan Nasional "Veteran" Jawa Timur, Surabaya, East Java, Indonesia

<sup>8</sup> Department of Chemistry, Faculty of Science and Data Analytics, Institut Teknologi Sepuluh Nopember, Keputih, Sukolilo, Surabaya, Indonesia; azizgb11@gmail.com;

\* Correspondence: setiawansyah@akfarcefada.ac.id (A.S.); azizgb11@gmail.com (A.A.);

Scopus Author ID 58628290500

Received: 25.01.2025; Accepted: 11.04.2025; Published: 8.06.2025

**Abstract:** Beta-caryophyllene is a sesquiterpene found in almost all plant essential oils that provide spacious biological activities. However, this compound is generally mixed with its isomers, leading to decreased caryophyllene purity. Rice husk offers a sustainable source of silica that can be doped with metal ions to increase the separation efficiency. This study aimed to synthesize metal ion-modified silica from rice husk and evaluate its effectiveness in separating beta-caryophyllene from its isomers. Silica was extracted and modified with metal ions (Al(NO<sub>3</sub>)<sub>3</sub>, CuSO<sub>4</sub>, FeNO<sub>3</sub>, and ZnNO<sub>3</sub>) using sol-gel and reflux methods. The resulting materials were characterized by XRD, FTIR, and SEM-EDX. XRD analysis confirmed the amorphous nature of the silica, indicated by the presence of a peak at 2θ 20-25°, while FTIR spectroscopy revealed the presence of characteristic silanol (O-H) and siloxane (Si-O-Si) groups. SEM-EDX analysis demonstrated successful metal ion doping and provided insights into the morphology and elemental composition of the modified silica, which indicated the presence of Al, Cu, Fe, and Zn with a round-ball form. The separation efficiency of the metal ion-modified silica was assessed using thin-layer chromatography (TLC) and gas chromatography-mass spectrometry (GC-MS). Al(NO<sub>3</sub>)<sub>3</sub>-modified silica showed the most promising results as a stationary phase for beta-caryophyllene purification. Column chromatography using this material achieved a 99% purity of beta-caryophyllene, as confirmed by GC-MS analysis. This study demonstrates the potential of metal ion-modified silica derived from rice husk as an effective and sustainable material for the separation of natural product isomers.

**Keywords:** synthesis; metal ion-modified silica; rice husk ash; beta-caryophyllene; isomer separation.

© 2025 by the authors. This article is an open-access article distributed under the terms and conditions of the Creative Commons Attribution (CC BY) license (<https://creativecommons.org/licenses/by/4.0/>), which permits unrestricted use, distribution, and reproduction in any medium, provided the original work is properly cited. The authors retain the copyright of

their work, and no permission is required from the authors or the publisher to reuse or distribute this article as long as proper attribution is given to the original source.

## 1. Introduction

The global demand for sustainable and eco-friendly materials has increased interest in agricultural waste valorization. Rice husk, a by-product of rice processing, presents a promising source of silica that can be modified for various applications [1]. Concurrently, the pharmaceutical and fragrance industries have shown a growing interest in separating and purifying natural compounds, particularly terpenes like beta-caryophyllene. Beta-caryophyllene, a sesquiterpene found in various essential oils, exhibits diverse biological activities, including anti-inflammatory [2,3], antioxidant [4], anti-hyperuricemia [5], and anticancer properties [6-9]. However, its natural form often exists as a mixture of isomers, presenting challenges in isolation and purification. Efficient separation of these isomers is crucial for enhancing the compound's efficacy and expanding potential applications.

Traditional separation methods often face limitations in terms of efficiency, cost, and environmental impact. For example, High-speed counter-current chromatography (HSCC) and metal ion-based counter-current chromatography (CCC) provide fairly good separation of isomeric compounds with a purity of 99% [10,11]. However, it is very difficult to maintain the liquid stationary phase in a steady state while the mobile phase flows through the stationary phase [12,13]. Additionally, HSCC and metal ion-based CCC are very difficult to use and require large amounts of samples [14]. Recent advancements in materials science have opened new avenues for developing novel adsorbents and separation media. Metal ion-modified silica has emerged as a promising material for selective adsorption and separation of organic compounds due to its tuneable surface properties and high specificity [15].

Modification of silica as a stationary phase for isomer separation generally uses silver ion-silica impregnation techniques. Li *et al.* [16] separated terpenoid and steroid compounds with a stationary phase of silver ion ( $\text{Ag}^{2+}$ ) impregnated silica. A similar study was also conducted by Setiawansyah *et al.* [17], who separated beta-caryophyllene from alpha-caryophyllene and caryophyllene oxide using TLC and classical column chromatography with silica- $\text{AgNO}_3$  as the stationary phase. This shows that the use of metals as silica modification materials has great potential. While extensive research has been conducted on silica-based adsorbents, synthesizing metal ion-modified silica from rice husk for isomer separation remains largely unexplored. Rice husks have a very high silica content, ranging from 85-99% [18-20]. Additionally, there have been no reports on using other metals in silica modification for isomer separation.

Therefore, this study aims to bridge this research gap by synthesizing metal ion-based modified silica from rice husk using various metal sources and investigating its application in the isomer separation of natural beta-caryophyllene. By addressing the dual challenges of agricultural waste utilization and efficient isomer separation, this research contributes to developing sustainable materials and advanced separation techniques with potential implications for the pharmaceutical, fragrance, and materials industries.

## 2. Materials and Methods

### 2.1. Chemicals and reagents.

Rice husk was obtained from Bandar Lampung, and clove oil was purchased from Darjeeling Sembrani Aroma, Indonesia. Beta-caryophyllene (purity 99% by GC) was kindly given by Dr. Muhammad Ikhlas Arsul, Department of Pharmacy, Universitas Islam Negeri Alauddin. Analytical grade of chemicals and reagents were also used in this study, including CuSO<sub>4</sub>, FeNO<sub>3</sub>, Al(NO<sub>3</sub>)<sub>3</sub>, ZnNO<sub>3</sub>, methanol, NaOH, HCl, n-hexane, ethyl acetate, acetic acid, H<sub>2</sub>SO<sub>4</sub>, and distilled water. All chemicals and reagents were purchased from Merck, Germany.

### 2.2. Synthesis of metal ion-modified silica from rice husk.

The synthesis of metal-ion-modified silica was employed based on the methods described by Ngatijo *et al.* [21] and Setiawansyah *et al.* [17] with modifications. Initially, rice husks were burned at 700°C to produce Rice Husk Ash (RHA). A mixture of RHA (100 g), sodium hydroxide (80 g), and water (500 mL) was stirred and refluxed at 100°C for 2 hours, then cooled and filtered. 2 M HCl was then added drop by drop carefully to the filtrate until the pH reached 9, forming a sol. This sol was aged for 3 days (3×24 hours) to form a silica gel. The silica gel was then washed until it reached a neutral pH, filtered, and dried at 70°C. Approximately 20 g of silica gel was mixed with 100 mL of metal-ion solution (10% CuSO<sub>4</sub>, 20% FeNO<sub>3</sub>, 10% Al(NO<sub>3</sub>)<sub>3</sub>, 10% ZnNO<sub>3</sub>) in a round bottom flask. The mixtures were then refluxed at 80°C for two hours and dried at 105°C for 1 hour.

### 2.3. Characterization of metal ion-modified silica.

Metal ion-modified silica synthesized from RHA using various metal ion sources underwent comprehensive characterization. Several analytical techniques were employed: Scanning electron microscope-energy dispersive X-ray (SEM-EDX) HITACHI FLEXSEM 100 identified the physical morphology along with chemical composition; Fourier-transform infrared spectrometry (FTIR) characterized organic bonds using a Fourier Transform – 1020 Spectrometer (Shimadzu, Japan), recorded at 4000–400 cm<sup>-1</sup>; X-ray diffraction (XRD) determined the amorphous nature of silica using an X-ray diffractometer (LynxEye) with CuKα radiation at 40 kV, 35 mA, and a 2θ scanning range from 2° to 50°.

### 2.4. Evaluation of isomer separation on metal ion-modified silica using TLC and column chromatography.

TLC plates were constructed by adhering the metal ion-modified silica on a 5 x 10 cm aluminum plate using gypsum solution. The metal ion-modified TLC silica plates were then activated in an oven at 100°C for 30 minutes prior to sample application. 2 μL beta-caryophyllene was applied as a 5 mm band on metal ion-modified TLC silica plates. Chromatographic separation was achieved through linear ascending development in a twin-trough chamber under saturated conditions, utilizing an n-hexane-ethyl acetate-acetic acid (7:3:0.1) solvent system. Post-development, the plate was derivatized using 10% (v/v) H<sub>2</sub>SO<sub>4</sub> in methanol, then heated at 100°C for 1 minute. Subsequent visualization was performed under visible light to analyze the separated components comprehensively.

The best metal ion-modified silica was further used for isolating beta-caryophyllene using classical column chromatography. A 50 g metal ion-modified silica was packed into a

column (length 20 cm, diameter 5 cm) using a wet packing technique. 1 g sample was then loaded into a packed column. The elution process was employed using n-hexane – ethyl acetate – acetic acid (7:3:0.1) as the mobile phase. The fractions were then collected and subjected to GC-MS analysis using GC-MS Agilent 7820A equipped with HP-5MS UI column silica (30 m × 0.25 mm×0.25 μm) (Agilent Technology, USA). GC-MS operation conditions were performed with an initial oven temperature of 90°C and 2°C per minute, increasing the temperature until the temperature reaches 150°C. The temperature was held for 20 min at 300°C. Elution was done using helium gas; the pressure was 166 kPa with 20 cms<sup>-1</sup> linear velocities; injector temperature 250°C; detector temperature 300°C; and split ratio 1:80.

### 3. Results and Discussion

#### 3.1. XRD analysis.

In this study, XRD analysis was conducted to determine the phase formed after the manufacture of modified silica gel with metal ions. The results of the XRD analysis are shown in Figure 1. The XRD diffractogram shows the formation of an amorphous phase, and there is a wide peak at 2theta 20-25° [22]. The detected peak formed is a typical peak of amorphous SiO<sub>2</sub>. All samples show similar results. There is only a slight shift, but still in the same range [23]. The XRD diffractogram after modification with metal ions shows the same peaks. No metal peaks appear. This can be caused by the small metal concentration and even the distribution of metal ions. However, the XRD results show that silica gel has been successfully made [24,25].

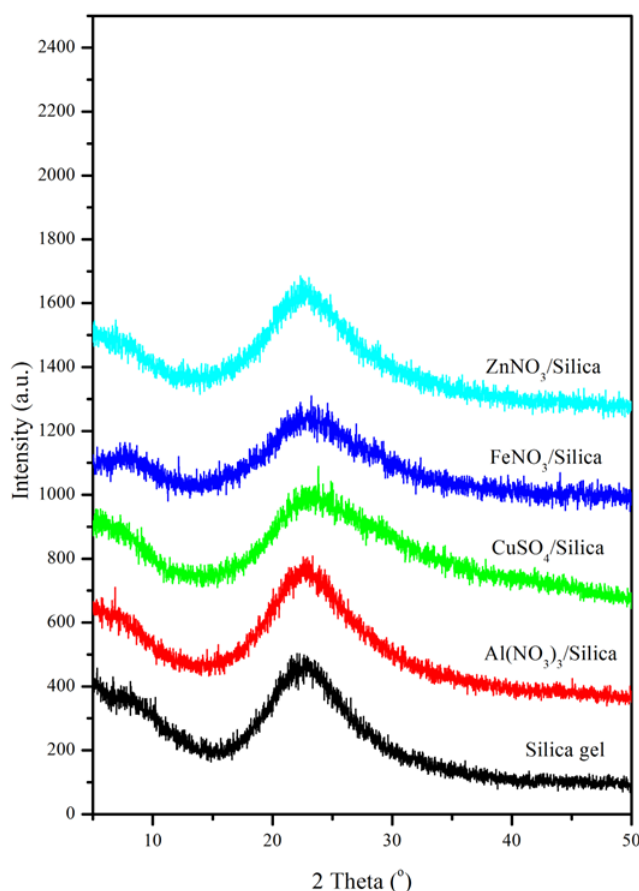


**Figure 1.** XRD pattern of various metal ion-based modified silica.

### 3.2. FT-IR analysis.

FTIR analysis was performed to see the functional groups present in the materials in the wavenumber range of 4000-400  $\text{cm}^{-1}$ . Figure 2 shows the FTIR results of silica gel and silica modified with various metal ions. The bands around 3500  $\text{cm}^{-1}$  show the O-H stretching of the silanol group (Si-OH) and absorbed water vapor. The peak around 1640  $\text{cm}^{-1}$  shows the O-H vibration of the water molecules absorbed [26]. The asymmetric stretching vibration of the siloxane group (Si-O-Si) appears at peaks around 1100 and 804  $\text{cm}^{-1}$ . The peak at around 940  $\text{cm}^{-1}$  indicates the asymmetric stretching vibration of the Si-O group [27]. FTIR results show that after modification of silica with metal ions, the peaks only showed a slight shift. The shift can be caused by the oxidation of functional groups and complex reactions between functional groups and metal ions [28].

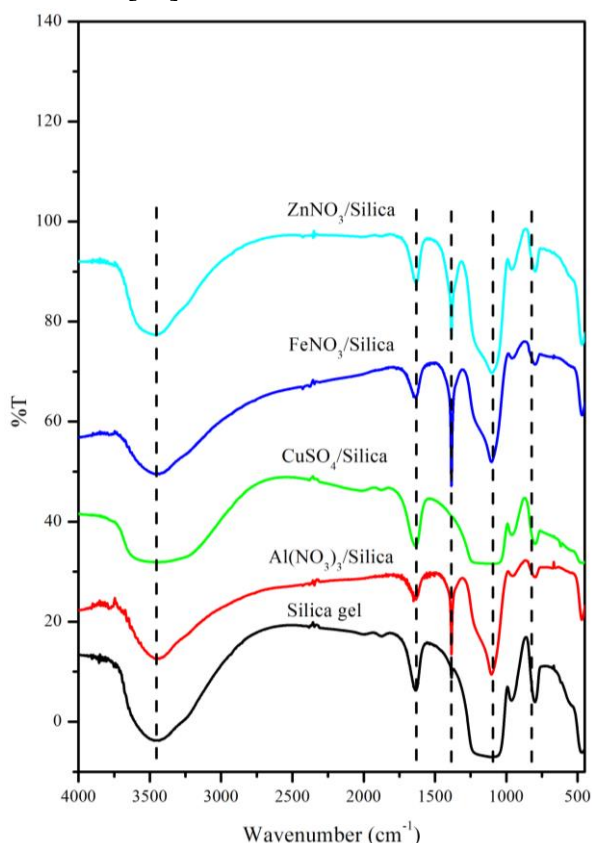


**Figure 2.** FTIR spectra of various metal ion-based modified silica.

### 3.3. SEM-EDX analysis.

Analysis with SEM-EDX was carried out to see the morphology formed and the composition of the elements contained in the material. Figure 3 shows an SEM image that shows similar morphology in all samples. The morphology of all materials is round, like a ball, and is evenly distributed [29]. The only difference is that the silica gel is smoother than the others because it's not modified by metal ions [30]. The silica gel sample modified by metal ions shows a round morphology, but the size is uneven, and metal is visible on the material's surface [31]. The difference in size and shape occurs due to the influence of the -OH group contained in the material. The more -OH groups there are, the smaller and rounder the uniform particles obtained. This is because the -OH group can bind to -Si- and reduce the carbon content [32].

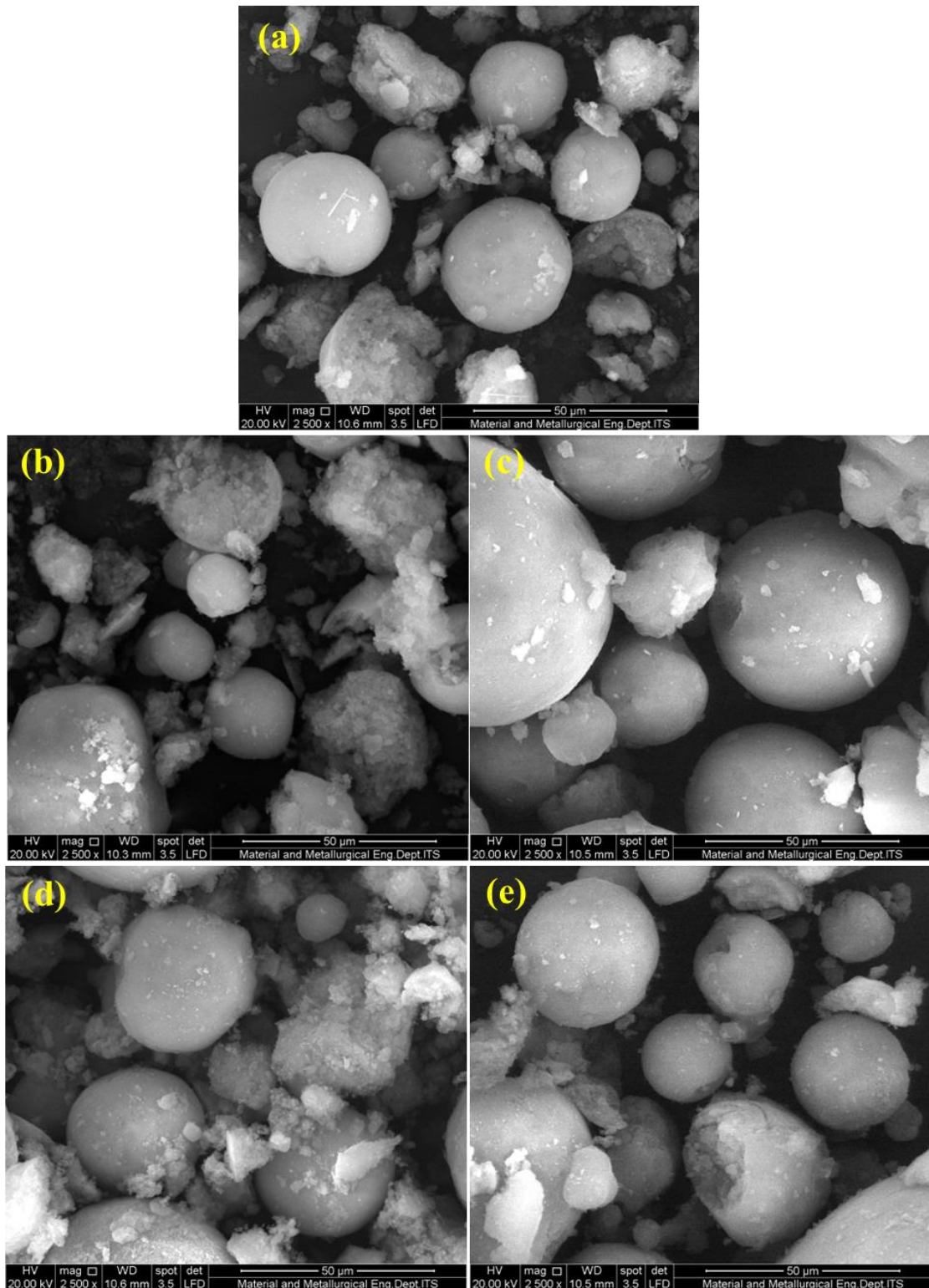


**Figure 3.** SEM images of (a) silica gel; (b)  $\text{Al}(\text{NO}_3)_3/\text{Silica}$ ; (c)  $\text{CuSO}_4/\text{Silica}$ ; (d)  $\text{FeNO}_3/\text{Silica}$ ; (e)  $\text{ZnNO}_3/\text{Silica}$ .

Particle size analysis was performed using ImageJ software based on SEM images. The particle size analysis results are shown in Figure 4, which shows inhomogeneous particle sizes. It can be seen that the particle size of silica gel is smaller than that of metal ion-modified silica gel [33]. This can be caused by agglomeration that occurs when doping with metal ions. The average particle size of metal ion doped silica is 10-50 µm, with silica gel having a particle size between 10-30 µm [34].

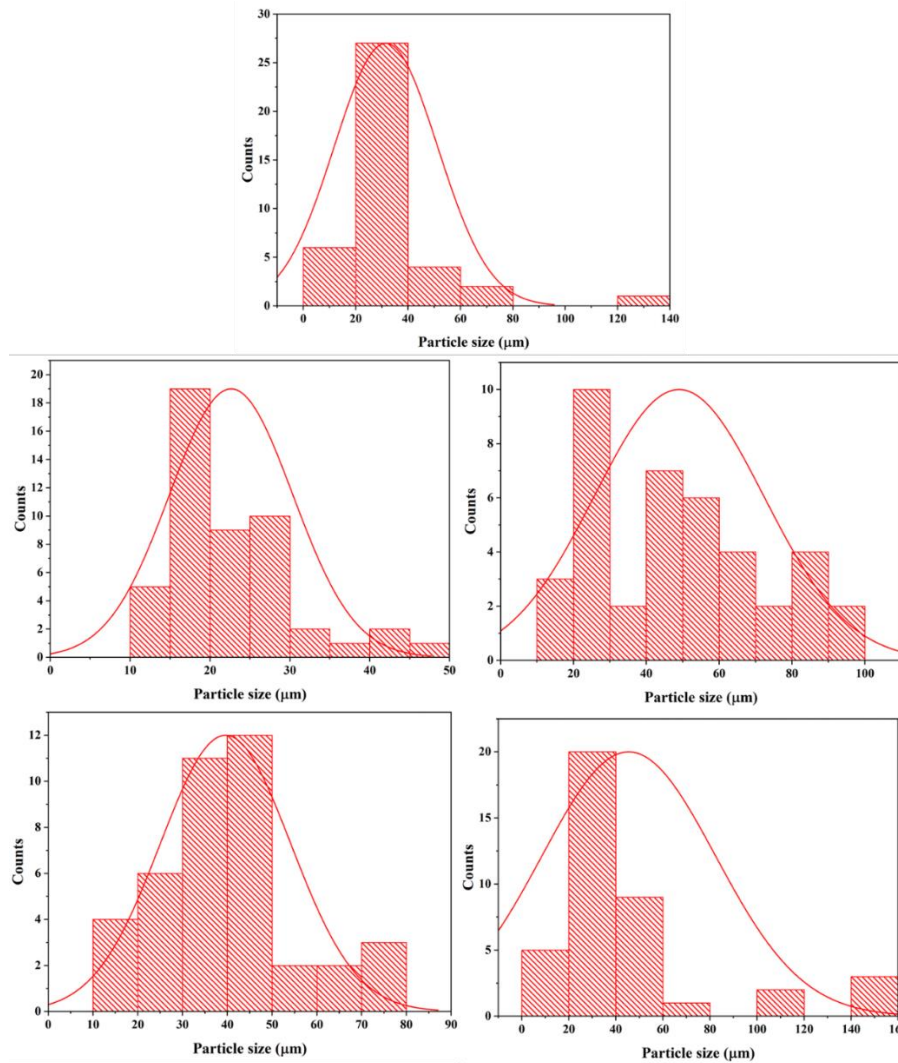


**Figure 4.** Particles sizes of (a) silica gel; (b) Al(NO<sub>3</sub>)<sub>3</sub>/Silica; (c) CuSO<sub>4</sub>/Silica; (d) FeNO<sub>3</sub>/Silica; (e) ZnNO<sub>3</sub>/Silica.

EDX analysis was conducted to determine the presence and composition of elements contained in metal ion-modified silica. The results of the EDX analysis are shown in Figure 5, which shows the EDX spectra, and in Table 1, which shows the elemental composition. The EDX results show the presence of all target elements present in the material. Metal peaks were detected in all spectra, and the elemental composition indicates the success of silica modification with metal ions [35]. The difference in the composition of each element can be caused by EDX displaying the composition according to the surface photographed in the SEM image, so it cannot show the elemental composition accurately. However, the results of the analysis with EDX can be used as a reference to state that the silica material has been modified with metal ions because of the appearance of peaks and the presence of target metals (Al, Cu, Fe, and Zn) in the material [36].

**Table 1.** EDX analysis of Element composition of metal ion-based modified silica.

Materials	Element Composition (%wt)								
	Si	O	N	Na	Al	Cu	Fe	Zn	S
Silica Gel	57.82	42.18	-	-	-	-	-	-	-
Al(NO <sub>3</sub> ) <sub>3</sub> /Silica	49.20	46.68	1.09	-	3.04	-	-	-	-
CuSO <sub>4</sub> /Silica	48.09	46.73	-	-	-	3.26	-	-	1.92
FeNO <sub>3</sub> /Silica	48.88	41.47	1.30	-	-	-	8.35	-	-
ZnNO <sub>3</sub> /Silica	45.51	43.42	1.57	4.52	-	-	-	4.98	-

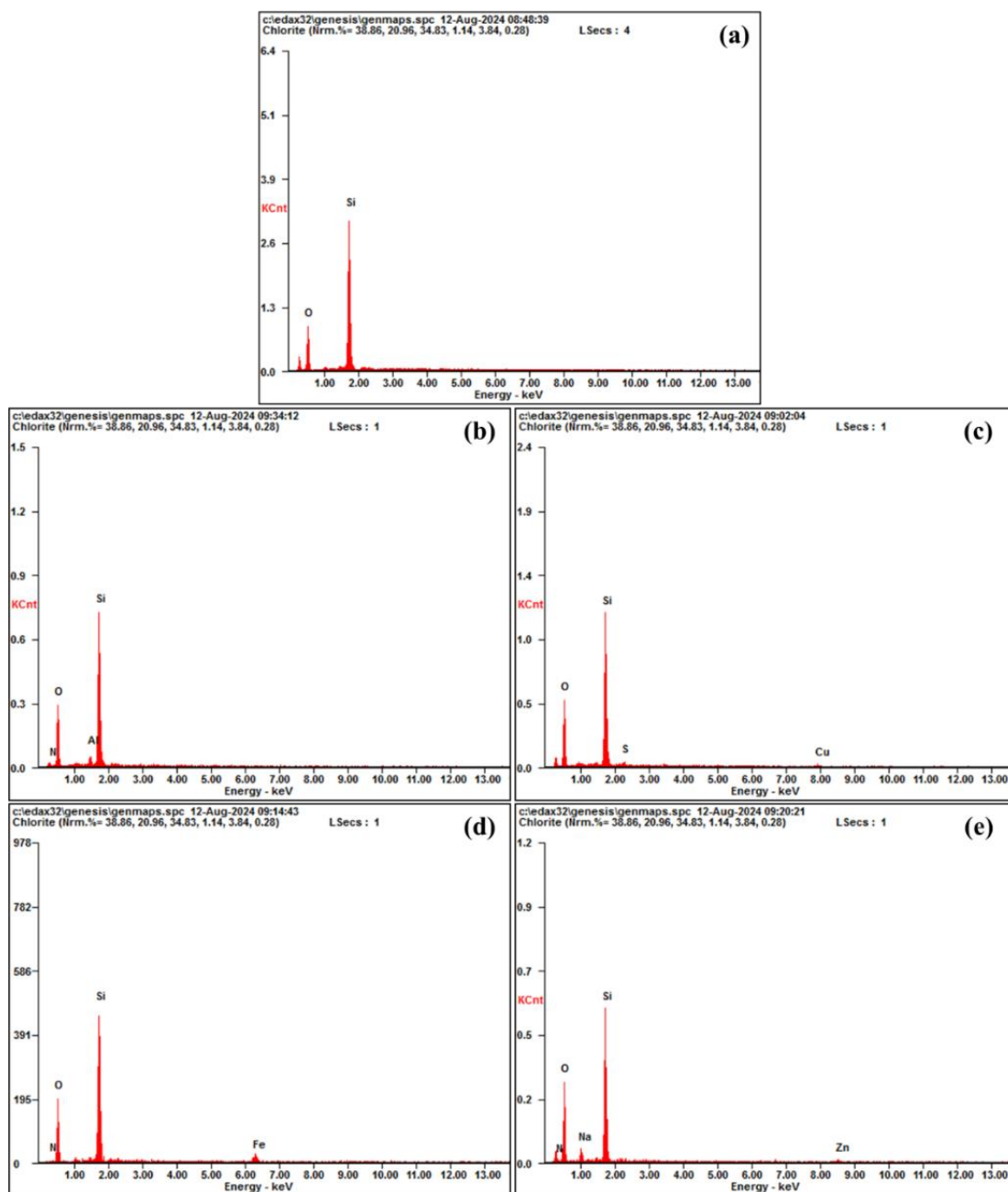


**Figure 5.** EDX element composition of (a) silica gel; (b) Al(NO<sub>3</sub>)<sub>3</sub>/Silica; (c) CuSO<sub>4</sub>/Silica; (d) FeNO<sub>3</sub>/Silica; (e) ZnNO<sub>3</sub>/Silica.

### 3.4. Evaluation of isomer separation on metal ion-modified silica using TLC and column chromatography.

Beta-caryophyllene was initially isolated from clove leaf essential oil using classical column chromatography. The GC-MS analysis of the initial isolate illustrated the obtained beta-caryophyllene was in low purity (50.71%), contaminated by its isomer, including alpha-caryophyllene (20.92%), caryophyllene oxide (13.90%), alpha-copaene (7.33%), and cadinene (7.14%) (Figure 6). TLC analysis in various metal ion-modified silica plates showed diverse results, in which the Al(NO<sub>3</sub>)<sub>3</sub> metal ion-modified silica stands as the most efficient stationary phase in separating beta-caryophyllene from the isomers. Even though other metal ion-modified silica provides separation, the isomers were not well-separated. Compared to other metal-ion modified silica, such as those using CuSO<sub>4</sub>, ZnNO<sub>3</sub>, and FeNO<sub>3</sub>, Al(NO<sub>3</sub>)<sub>3</sub> modified silica demonstrates superior separation capabilities, evidenced by the observation of four well-

separated spots as opposed to just two (Figure 7). This made  $\text{Al}(\text{NO}_3)_3$  modified silica subjected as column chromatography stationary phase for purification of beta-caryophyllene. A total of 25 fractions were obtained, in which fractions 4 – 9 were considered beta-caryophyllene fractions. GC-MS analysis (Figure 8) revealed that fractions 4 – 9 contained high-purity beta-caryophyllene (99%) that was free from its isomer.

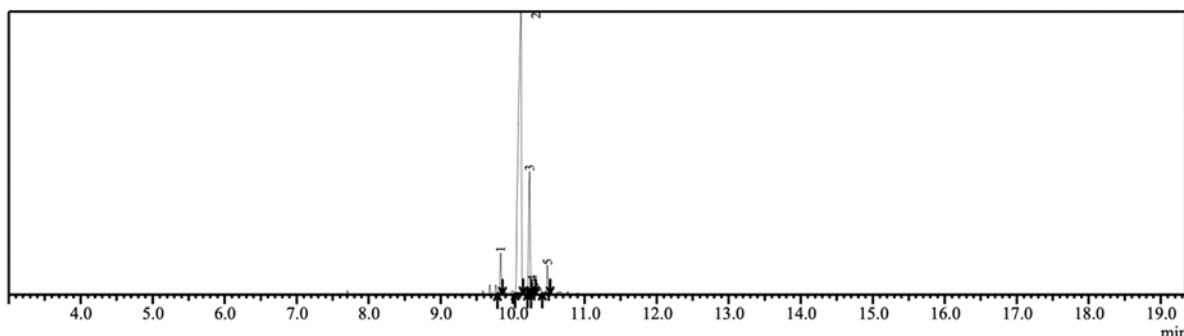


**Figure 6.** GC chromatogram of unpurified beta-caryophyllene.

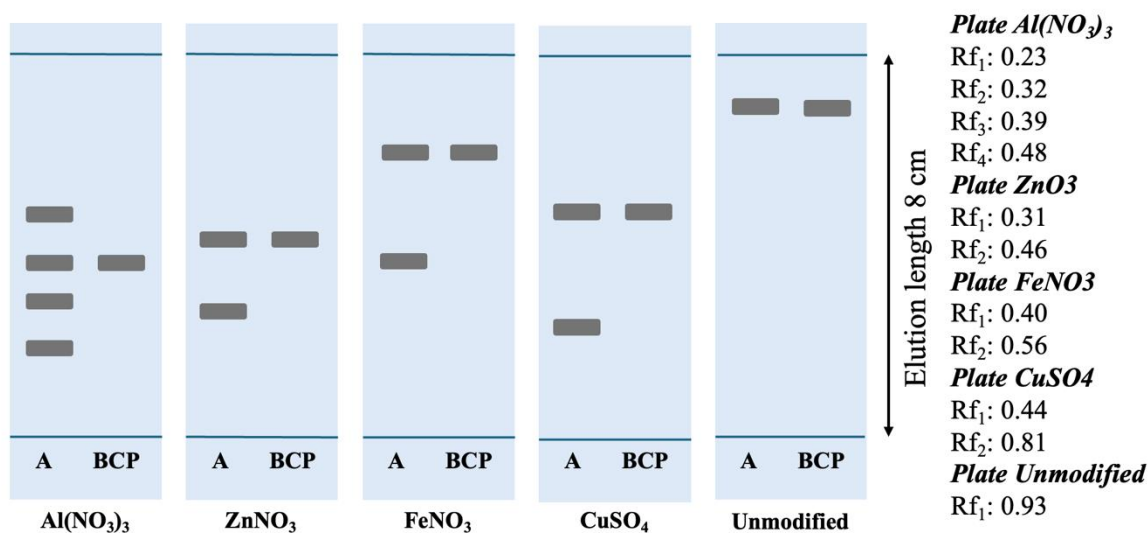


**Figure 7.** Illustration of TLC chromatogram in various TLC plates derivatized with 10% v/v  $\text{H}_2\text{SO}_4$  in methanol under visible light. Note: A, unpurified beta-caryophyllene; and BCP, pure beta-caryophyllene.

The enhanced performance of  $\text{Al}(\text{NO}_3)_3$ -modified silica can be attributed to the unique physicochemical properties of  $\text{Al}(\text{NO}_3)_3$  and its interactions with the silica surface. The specificity of  $\text{Al}(\text{NO}_3)_3$  modified silica in separating beta-caryophyllene from alpha-caryophyllene, caryophyllene oxide, alpha-copaene, and cadinene showcases the complex interplay of various molecular interactions in chromatographic separations.

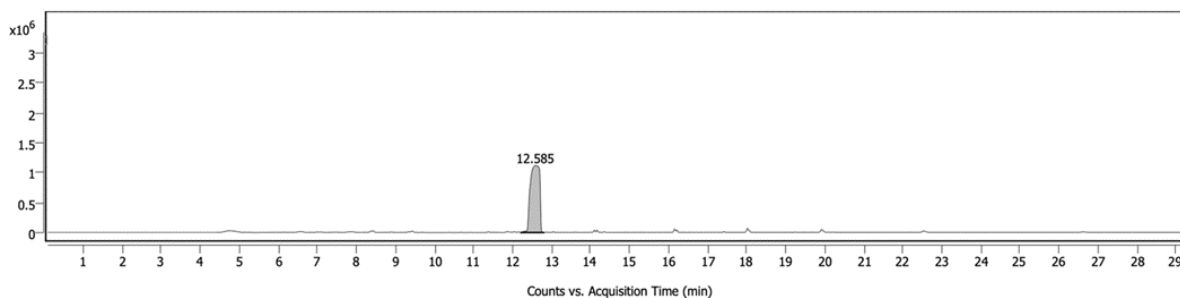


**Figure 8.** GC chromatogram of purified beta-caryophyllene

$\text{Al}^{3+}$  ions, characterized by their small ionic radius, high charge density, and strong Lewis acidity, likely form more stable and diverse coordination complexes with the oxygen-

<https://biointerfaceresearch.com/>

containing functional groups of caryophyllene compounds [37]. This interaction is particularly relevant for caryophyllene oxide, which contains an epoxide group. The surface morphology resulting from  $\text{Al}(\text{NO}_3)_3$  modification may create a more suitable environment for differentiation between these structurally similar molecules, possibly due to a combination of factors, including pore size distribution, surface area, and the specific arrangement of  $\text{Al}^{3+}$  ions on the silica surface [38,39].

Hydrophobic interactions play a crucial role in the separation process, especially for beta- and alpha-caryophyllene, which are hydrophobic sesquiterpenes. The  $\text{Al}(\text{NO}_3)_3$  modification likely creates regions of varying hydrophobicity on the silica surface, allowing for differential retention of the caryophyllene isomers based on their slight structural differences, as visualized in Figure 9 [13]. The four-ring structure of caryophyllene compounds also facilitates  $\pi$ - $\pi$  interactions, which can contribute significantly to the separation mechanism, in which the number of double bonds influences the interaction that occurs [40,41]. The presence of  $\text{Al}^{3+}$  ions may induce polarization in the  $\pi$ -electron systems of the caryophyllene molecules, enhancing  $\pi$ - $\pi$  interactions with the modified silica surface or with other caryophyllene molecules, leading to more nuanced separation [42]. The selectivity of  $\text{Al}(\text{NO}_3)_3$  modified silica might stem from its ability to simultaneously engage in multiple types of interactions - coordination with  $\text{Al}^{3+}$ , hydrophobic interactions, and  $\pi$ - $\pi$  interactions - creating a unique separation environment. The observation of four spots suggests that this combination of interactions allows the  $\text{Al}(\text{NO}_3)_3$  modified silica to distinguish subtle structural differences among the caryophyllene compounds, including potential conformational isomers or varying degrees of oxidation.

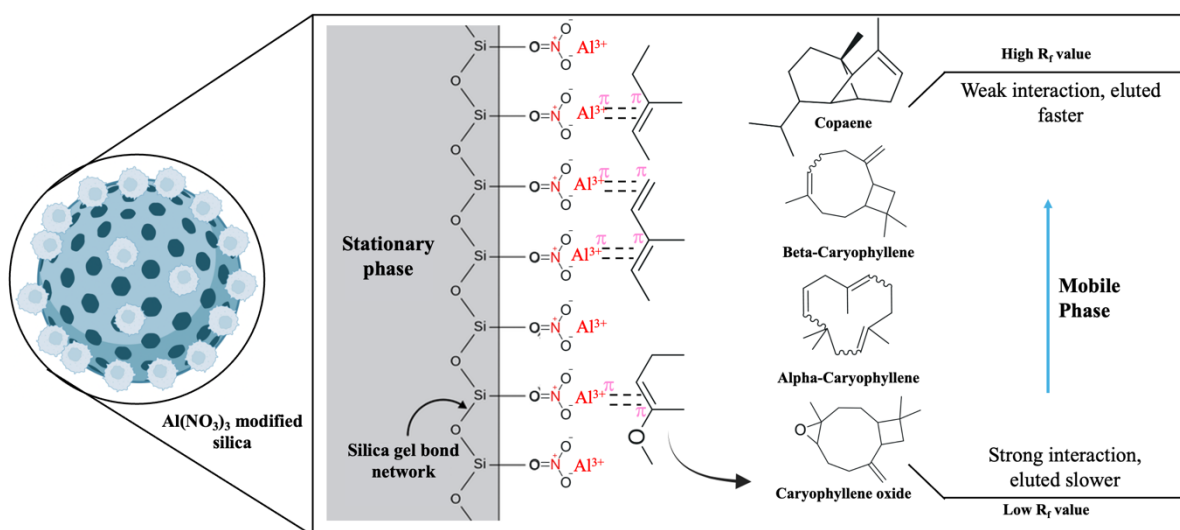


**Figure 9.** Schematic illustration of separation mechanism of beta-caryophyllene isomers on  $\text{Al}(\text{NO}_3)_3$  modified silica.

#### 4. Conclusions

Extraction and modification of silica with metal ions have been successfully carried out using sol-gel and reflux methods. The success of the extraction of metal ion-doped silica was confirmed by the characterization results using XRD, FTIR, and SEM-EDX. The XRD results showed a typical diffractogram of amorphous silica with a peak at  $2\theta$  20-25°. The FTIR results indicated the formation of silica material with typical silanol (Si-OH) and siloxane (Si-O-Si) peaks. The SEM-EDX results showed the success of metal ion doping with morphological forms and elemental compositions, indicating the presence of Al, Cu, Fe, and

Zn. The effectiveness of metal ion-modified silica for beta-caryophyllene purification has been tested using TLC and column chromatography techniques. Among the metal ion modifications, Al(NO<sub>3</sub>)<sub>3</sub>-modified silica showed superior performance as a stationary phase for beta-caryophyllene purification, achieving 99% purity. These findings highlight the potential of agricultural waste valorization for producing advanced materials with practical applications in natural product chemistry. Future research directions could include optimizing synthesis conditions to enhance separation efficiency, exploring the material's effectiveness with other natural product isomers, investigating scale-up potential for industrial applications, and conducting comprehensive sustainability assessments. These future directions aim to advance sustainable materials synthesis and their applications in separation science, potentially leading to more efficient and environmentally friendly processes in the pharmaceutical and natural product industries.

### **Author Contributions**

Conceptualization, A.S.; methodology, A.S. and A.A.; software, —; validation, A.S., A.A., A.U.P., Y.P., and R.E.N.; formal analysis, A.A.; investigation, S.P., J.E., Y.S., and W.K.; resources, —; data curation, S.P., J.E., Y.S., and W.K.; writing—original draft preparation, A.S.; writing—review and editing, A.A., Y.E.C., A.U.P., Y.P., K., M.A.M., and R.E.N.; visualization, —; supervision, A.S.; project administration, —; funding acquisition, R.E.N. All authors have read and agreed to the published version of the manuscript.

### **Institutional Review Board Statement**

Not applicable.

### **Informed Consent Statement**

Not applicable.

### **Data Availability Statement**

Data supporting the findings of this study are available upon reasonable request from the corresponding author.

### **Funding**

This research received no external funding.

### **Acknowledgments**

The authors would like to acknowledge Dr. Muhammad Ikhlas Arsul, Department of Pharmacy, Universitas Islam Negeri Alauddin, for providing standard beta-caryophyllene.

### **Conflicts of Interest**

The authors declare no conflict of interest.

## References

1. Pode, R. Potential Applications of Rice Husk Ash Waste from Rice Husk Biomass Power Plant. *Renewable and Sustainable Energy Reviews* **2016**, *53*, 1468–1485, doi:10.1016/j.rser.2015.09.051.
2. Ojha, S.; Javed, H.; Azimullah, S.; Haque, M.E.  $\beta$ -Caryophyllene, a Phytocannabinoid Attenuates Oxidative Stress, Neuroinflammation, Glial Activation, and Salvages Dopaminergic Neurons in a Rat Model of Parkinson Disease. *Mol Cell Biochem* **2016**, *418*, 59–70, doi:10.1007/s11010-016-2733-y.
3. Youssef, D.A.; El-Fayoumi, H.M.; Mahmoud, M.F. Beta-Caryophyllene Protects against Diet-Induced Dyslipidemia and Vascular Inflammation in Rats: Involvement of CB2 and PPAR- $\gamma$  Receptors. *Chem Biol Interact* **2019**, *297*, 16–24, doi:10.1016/j.cbi.2018.10.010.
4. Dahham, S.S.; Tabana, Y.M.; Iqbal, M.A.; Ahamed, M.B.K.; Ezzat, M.O.; Majid, A.S.A.; Majid, A.M.S.A. The Anticancer, Antioxidant and Antimicrobial Properties of the Sesquiterpene  $\beta$ -Caryophyllene from the Essential Oil of *Aquilaria Crassna*. *Molecules* **2015**, *20*, 11808–11829, doi:10.3390/molecules200711808.
5. Setiawansyah, A.; Gemantari, B.M. Potential Activity of Caryophyllene Derivatives as Xanthine Oxidase Inhibitor: An in Silico Quantitative Structure-Activity Relationship Analysis. *Journal of Food and Pharmaceutical Sciences* **2022**, *10*, 700–708, doi:10.22146/jfps.5485.
6. Francomano, F.; Caruso, A.; Barbarossa, A.; Fazio, A.; La Torre, C.; Llamaci, R.; Saturnino, C.; Iacopetta, D.; Sinicropi, Maria SCeramella, J.; Matefania  $\beta$ -Caryophyllene a Sesquiterpene with Countless. *Applied Sciences* **2019**, *9*, 5420–5438.
7. Fidy, K.; Fiedorowicz, A.; Strzadala, L.; Szumny, A. B-Caryophyllene and B-Caryophyllene Oxide—Natural Compounds of Anticancer and Analgesic Properties. *Cancer Med* **2016**, *5*, 3007–3017, doi:10.1002/cam4.816.
8. Amiel, E.; Ofir, R.; Dudai, N.; Soloway, E.; Rabinsky, T.; Rachmilevitch, S.  $\beta$ -Caryophyllene, a Compound Isolated from the Biblical Balm of Gilead (*Commiphora Gileadensis*), Is a Selective Apoptosis Inducer for Tumor Cell Lines. *Evidence-based Complementary and Alternative Medicine* **2012**, *2012*, doi:10.1155/2012/872394.
9. Zhou, L.; Zhan, M.L.; Tang, Y.; Xiao, M.; Li, M.; Li, Q.S.; Yang, L.; Li, X.; Chen, W.W.; Wang, Y.L. Effects of  $\beta$ -Caryophyllene on Arginine ADP-Ribosyltransferase 1-Mediated Regulation of Glycolysis in Colorectal Cancer under High-Glucose Conditions. *Int J Oncol* **2018**, *53*, 1613–1624, doi:10.3892/ijo.2018.4506.
10. Yun W, Jilin D. Method for separating and preparing caryophyllene oxide, beta-farnesene and caryophyllene [Internet]. China: Google Patent; CN102603458B, **2012**. Available from: <https://patents.google.com/patent/CN102603458B/en>.
11. Han, C.; Wang, W.; Xue, G.; Xu, D.; Zhu, T.; Wang, S.; Cai, P.; Luo, J.; Kong, L. Metal Ion-Improved Complexation Counter-current Chromatography for Enantioseparation of Dihydroflavone Enantiomers. *J Chromatogr A* **2018**, *1532*, 1–9, doi:10.1016/j.chroma.2017.12.006.
12. Ma, L.; Li, Y.; Shang, L.; Ma, Y.; Sun, Y.; Ji, W. Preparation of Sp<sup>2c</sup>-COF Functionalized Silica Gel Material as Chromatographic Stationary Phases for Their High-Resolution Separation of Geometric Isomers. *Microchemical Journal* **2024**, *206*, doi:10.1016/j.microc.2024.111569.
13. Berthod, A.; Maryutina, T.; Spivakov, B.; Shpigun, O.; Sutherland, I.A. Counter-current Chromatography in Analytical Chemistry (IUPAC Technical Report). *Pure and Applied Chemistry* **2009**, *81*, 355–387, doi:10.1351/PAC-REP-08-06-05.
14. Sethi, N.; Anand, A.; Sharma, A.; Chandrul, K.; Jain, G.; Srinivasa, K. High Speed Counter Current Chromatography: A Support-Free LC Technique. *J Pharm Bioallied Sci* **2009**, *1*, 8, doi:10.4103/0975-7406.62680.
15. Soltani, R.; Marjani, A.; Hosseini, M.; Shirazian, S. Synthesis and Characterization of Novel N-Methylimidazolium-Functionalized KCC-1: A Highly Efficient Anion Exchanger of Hexavalent Chromium. *Chemosphere* **2020**, *239*, 124735, doi:10.1016/j.chemosphere.2019.124735.
16. Li, T.S.; Li, J.T.; Li, H.Z. Modified and Convenient Preparation of Silica Impregnated with Silver Nitrate and Its Application to the Separation of Steroids and Triterpenes. *J Chromatogr A* **1995**, *715*, 372–375, doi:10.1016/0021-9673(95)00619-X.
17. Setiawansyah, A.; Arsul, M.I.; Sukrasno, S.; Damayanti, S.; Insanu, M.; Fidrianny, I. Anti-Hyperuricemic Potential of Caryophyllene from *Syzygium Aromaticum* Essential Oil: SiO<sub>2</sub>-AgNO<sub>3</sub>-Based Column Chromatography Purification, Antioxidant, and Xanthine Oxidase Inhibitory Activities. *Advances in Traditional Medicine* **2024**, *24*, 475–487, doi:10.1007/s13596-023-00710-5.

18. Novembre, D.; Gimeno, D.; Marinangeli, L.; Tangari, A.C.; Rosatelli, G.; Ciulla, M.; Profio, P. Rice Husk as Raw Material in Synthesis of NaA (LTA) Zeolite. **2024**, 1–14.
19. Gebretatios, A.G.; Kadiri Kanakka Pillantakath, A.R.; Witoon, T.; Lim, J.W.; Banat, F.; Cheng, C.K. Rice Husk Waste into Various Template-Engineered Mesoporous Silica Materials for Different Applications: A Comprehensive Review on Recent Developments. *Chemosphere* **2023**, *310*, 136843, doi:10.1016/j.chemosphere.2022.136843.
20. Kamari, S.; Ghorbani, F. Extraction of Highly Pure Silica from Rice Husk as an Agricultural By-Product and Its Application in the Production of Magnetic Mesoporous Silica MCM-41. *Biomass Convers Biorefin* **2021**, *11*, 3001–3009, doi:10.1007/s13399-020-00637-w.
21. Ngatijo; Basuki, R.; Rusdiarso, B.; Nuryono Sorption-Desorption Profile of Au(III) onto Silica Modified Quaternary Amines (SMQA) in Gold Mining Effluent. *J Environ Chem Eng* **2020**, *8*, doi:10.1016/j.jece.2020.103747.
22. Wang, X.; Han, X.; Kang, L.; Feng, S.; Wang, M.; Wang, Y.; Huang, S.; Zhao, Y.; Wang, S.; Ma, X. Regulating Electronic Environment on Alkali Metal-Doped Cu@NS-SiO<sub>2</sub> for Selective Anisole Hydrodeoxygenation. *Green Chemical Engineering* **2023**, *4*, 294–302, doi:10.1016/j.gce.2022.06.003.
23. Wu, X.; Chai, F.; Yang, J.; Li, Y.; Wu, X.; Chen, P. Artificial Aluminum-Doped SiO<sub>2</sub> Aerogel Coating Layer Regulating Zinc Ions Flow for Highly Reversible Dendrite-Free Zinc Anodes. *Electrochim Acta* **2024**, *501*, 144799, doi:10.1016/j.electacta.2024.144799.
24. Hernández, M.A.; González, A.I.; Corona, L.; Hernández, F.; Rojas, F.; Asomoza, M.; Solís, S.; Portillo, R.; Salgado, M.A. Chlorobenzene, Chloroform, and Carbon Tetrachloride Adsorption on Undoped and Metal-Doped Sol-Gel Substrates (SiO<sub>2</sub>, Ag/SiO<sub>2</sub>, Cu/SiO<sub>2</sub> and Fe/SiO<sub>2</sub>). *J Hazard Mater* **2009**, *162*, 254–263, doi:10.1016/j.jhazmat.2008.05.051.
25. Adegoke, O.; Oyinlola, K.; Achadu, O.J.; Yang, Z. Blue-Emitting SiO<sub>2</sub>-Coated Si-Doped ZnSeS Quantum Dots Conjugated Aptamer-Molecular Beacon as an Electrochemical and Metal-Enhanced Fluorescence Biosensor for SARS-CoV-2 Spike Protein. *Anal Chim Acta* **2023**, *1281*, 341926, doi:10.1016/j.aca.2023.341926.
26. Mekprasart, W.; Songpanit, M.; Sanyen, T.; Samart, S.; Chutipaijit, S.; Pecharapa, W.; Boonyarattanakalin, K. X-Ray Characterization, Structural Analysis, Antibacterial Activity, and Self-Cleaning Property of Cu-Doped TiO<sub>2</sub>-SiO<sub>2</sub> Nanocomposite Prepared by Sonochemical Process. *Radiation Physics and Chemistry* **2024**, *225*, 112147, doi:10.1016/j.radphyschem.2024.112147.
27. De Silva, A.U.T.; Cooray, A.T.; Kumarasinghe, K.G.U.R. Silica-Supported Indole Derived Fluorometric Chemosensor for the Selective Detection of Ag<sup>+</sup> Ions in Aqueous Solution. *Journal of the Indian Chemical Society* **2024**, *101*, 101154, doi:10.1016/j.jics.2024.101154.
28. Díaz-Muñoz, L.L.; Bonilla-Petriciolet, A.; Reynel-Ávila, H.E.; Mendoza-Castillo, D.I. Sorption of Heavy Metal Ions from Aqueous Solution Using Acid-Treated Avocado Kernel Seeds and Its FTIR Spectroscopy Characterization. *J Mol Liq* **2016**, *215*, 555–564, doi:10.1016/j.molliq.2016.01.022.
29. Sarkar, S.M.; Rahman, M.L. Silica Gel-Supported Pd Nanocatalyst: Efficient Mizoroki-Heck Reactions and Sustainable Ozagrel Synthesis. *Giant* **2024**, *19*, 100326, doi:10.1016/j.giant.2024.100326.
30. Song, Z.; Li, S.; Guan, Y.; Wang, S.; Wang, Y.; Yang, G.; Zhang, X.; Li, J.; Song, W.; Zhou, C.; *et al.* Facile Synthesis of Zirconia-Coated Mesoporous Silica Particles by Hydrothermal Strategy under Low Potential of Hydrogen Conditions and Functionalization with Dodecylphosphonic Acid for High-Performance Liquid Chromatography. *J Chromatogr A* **2020**, *1612*, doi:10.1016/j.chroma.2019.460659.
31. Imoisili, P.E.; Jen, T.-C. Synthesis and Characterization of Amorphous Nano Silica from South African Coal Fly Ash. *Mater Today Proc* **2023**, *0–5*, doi:10.1016/j.matpr.2023.06.077.
32. Zushi, R.; Hayashi, Y.; Yamanaka, T.; Takizawa, H. Facile Room Temperature Synthesis of Size-Controlled Spherical Silica from Silicon Metal via Simple Sonochemical Process. *Ultrason Sonochem* **2024**, *107*, 106913, doi:10.1016/j.ultsonch.2024.106913.
33. Aziz, A.; Andini Putri, B.G.; Prasetyoko, D.; Nugraha, R.E.; Holilah, H.; Bahruji, H.; Jalil, A.A.; Suprpto, S.; Hartati, H.; Asikin-Mijan, N. Synthesis of Mesoporous Zeolite Y Using Sapindus Rarak Extract as Natural Organic Surfactant for Deoxygenation of Reutealis Trisperma Oil to Biofuel. *RSC Adv* **2023**, *13*, 32648–32659, doi:10.1039/d3ra05390c.
34. Mohamed, A.L.; Khattab, T.A.; Rehan, M.F.; Hassabo, A.G. Mesoporous Silica Encapsulating ZnS Nanoparticles Doped Cu or Mn Ions for Warning Clothes. *Results Chem* **2023**, *5*, 100689, doi:10.1016/j.rechem.2022.100689.

35. Sabeena, G.; Rajadurai, S.; bala, S.P.M.; Manju, T.; Alhadlaq, H.A.; Mohan, R.; Annadurai, G.; Ahamed, M. In Vitro Antidiabetic and Anti-Inflammatory Effects of Fe-Doped CuO-Rice Husk Silica (Fe-CuO-SiO<sub>2</sub>) Nanocomposites and Their Enhanced Innate Immunity in Zebrafish. *J King Saud Univ Sci* **2022**, *34*, 102121, doi:10.1016/j.jksus.2022.102121.
36. Mende, M.; Schwarz, D.; Steinbach, C.; Boldt, R.; Schwarz, S. Colloids and Surfaces A : Physicochemical and Engineering Aspects Simultaneous Adsorption of Heavy Metal Ions and Anions from Aqueous Solutions on Chitosan — Investigated by Spectrophotometry and SEM-EDX Analysis. *Colloids Surf A Physicochem Eng Asp* **2016**, *510*, 275–282, doi:10.1016/j.colsurfa.2016.08.033.
37. Xu, M.; Wang, W.; Seiler, M.; Buchholz, A.; Hunger, M. Improved Brønsted Acidity of Mesoporous [Al]MCM-41 Material Treated with Ammonium Fluoride. *Journal of Physical Chemistry B* **2002**, *106*, 3202–3208, doi:10.1021/jp014222a.
38. Samriani, S.; Zakir, M.; Taba, P.; La Nafie, N.; Indriani, I. Synthesis of MCM-41 Silica Mesoporous Modified with Zn Metal. *Jurnal Kimia Sains dan Aplikasi* **2022**, *25*, 286–291, doi:10.14710/jksa.25.8.286-291.
39. Shvets, O.; Belyakova, L. Synthesis, Characterization and Sorption Properties of Silica Modified with Some Derivatives of  $\beta$ -Cyclodextrin. *J Hazard Mater* **2015**, *283*, 643–656, doi:10.1016/j.jhazmat.2014.10.012.
40. Morris, L.J. Separations of Lipids by Silver Ion Chromatography. *J Lipid Res* **1966**, *7*, 717–732, doi:10.1016/s0022-2275(20)38948-3.
41. Mander, L.N.; Williams, C.M. Chromatography with Silver Nitrate: Part 2. *Tetrahedron* **2016**, *72*, 1133–1150, doi:10.1016/j.tet.2016.01.004.
42. Verstraeten, S. V.; Oteiza, P.I. Effects of Al<sup>3+</sup> and Related Metals on Membrane Phase State and Hydration: Correlation with Lipid Oxidation. *Arch Biochem Biophys* **2000**, *375*, 340–346, doi:10.1006/abbi.1999.1671.

### **Publisher’s Note & Disclaimer**

The statements, opinions, and data presented in this publication are solely those of the individual author(s) and contributor(s) and do not necessarily reflect the views of the publisher and/or the editor(s). The publisher and/or the editor(s) disclaim any responsibility for the accuracy, completeness, or reliability of the content. Neither the publisher nor the editor(s) assume any legal liability for any errors, omissions, or consequences arising from the use of the information presented in this publication. Furthermore, the publisher and/or the editor(s) disclaim any liability for any injury, damage, or loss to persons or property that may result from the use of any ideas, methods, instructions, or products mentioned in the content. Readers are encouraged to independently verify any information before relying on it, and the publisher assumes no responsibility for any consequences arising from the use of materials contained in this publication.